Interplay between Barrier Width and Height in Electron Tunneling: Photoinduced Electron Transfer in Porphyrin-Based Donor−Bridge−Acceptor Systems

Karin Pettersson,[†] Joanna Wiberg,[†] Thomas Ljungdahl,[‡] Jerker Mårtensson,[‡] and Bo Albinsson*,[†]

Department of Chemical and Biological Engineering/Physical Chemistry and -Organic Chemistry, Chalmers University of Technology, SE-412 96 Göteborg, Sweden

Received: August 8, 2005; In Final Form: October 14, 2005

The rate of electron tunneling in molecular donor−bridge−acceptor (D−B−A) systems is determined both by the tunneling barrier width and height, that is, both by the distance between the donor and acceptor as well as by the energy gap between the donor and bridge moieties. These factors are therefore important to control when designing functional electron transfer systems, such as constructs for photovoltaics, artificial photosynthesis, and molecular scale electronics. In this paper we have investigated a set of D−B−A systems in which the distance and the energy difference between the donor and bridge states (ΔE_{DB}) are systematically varied. Zinc(II) and gold(III) porphyrins were chosen as electron donor and acceptor because of their suitable driving force for photoinduced electron transfer (−0.9 eV in butyronitrile) and well-characterized photophysics. We have previously shown, in accordance with the superexchange mechanism for electron transfer, that the electron transfer rate is proportional to the inverse of ΔE_{DB} in a series of zinc/gold porphyrin D−B−A systems with bridges of constant edge to edge distance (19.6 Å) and varying ΔE_{DB} (3900−17 600 cm^{-1}). Here, we use the same donor and acceptor but the bridge is shortened or extended giving a set of oligo-*p*-phenyleneethynylene bridges (OPE) with four different edge to edge distances ranging from 12.7 to 33.4 Å. These two sets of D−B−A systems—ZnP−RB−AuP^+ and ZnP−nB−AuP^+—have one bridge in common, and hence, for the first time both the distance and ΔE_{DB} dependence of electron transfer can be studied simultaneously in a systematic way.

Introduction

The probability of quantum mechanical tunneling depends on the energy and mass of the particle and on the height (ΔE_{DB}) and width (R_{DA}) of the barrier. In this way electron transfer in a donor−bridge−acceptor (D−B−A) system can be pictured, where the barrier height is the energy splitting between the relevant states of the donor and bridge (ΔE_{DB}), and the barrier width the distance between donor and acceptor (R_{DA}) (Figure 1). Electron tunneling has exponential distance dependence as well as inverse dependence on the barrier height which for electron transfer in a D−B−A system is expressed by the superexchange mechanism.[1,2] Primarily, the distance dependence of electron transfer has been studied[3−7] but also the energy splitting dependence.[8,9] To our knowledge, studying both at the same time in a systematic way has not yet been done. We have constructed two sets of D−B−A systems ZnP−RB−AuP^+ and ZnP−nB−AuP^+ (Figure 2), which gives us a unique possibility to study how electron transfer depends both on the distance and the energy splitting at the same time.

As model compounds we have chosen a suitable electron transfer donor−acceptor couple,[10−12] zinc(II) 5,15-diaryl-2,8,-12,18-tetraethyl-3,7,13,17-tetramethylporphyrin (ZnP) and the corresponding gold(III) tetrafluoroborate porphyrin (AuP^+),

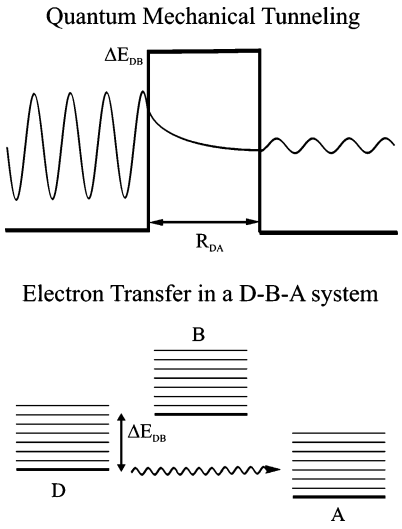

Figure 1. Schematic comparison of quantum mechanical tunneling and electron transfer in a D−B−A system.

respectively. Previously we have studied electron transfer in ZnP−RB−AuP^+ systems where the bridges (RB, R = O, 3, N, and A) were of equal length but had different electronic properties.[9] The bridges were 1,4-bis(phenylethynyl)bicyclo-octane (OB), 1,4-bis(phenylethynyl)benzene (3B), 1,4-bis-(phenylethynyl)naphthalene (NB), and 9,10-bis(phenylethynyl)-anthracene (AB); see Figure 2. By keeping the distance constant — center-to-center R_{cc} = 26.5 Å — the differences of the measured electron-transfer rates could be attributed to the

* Corresponding author. Phone: +46 31 772 30 44. Fax: +46 31 772 38 58. E-mail: balb@chalmers.se.
[†] Department of Chemical and Biological Engineering/Physical Chemistry.
[‡] Department of Chemical and Biological Engineering/Organic Chemistry.

10.1021/jp054420s CCC: $33.50
Published on Web 12/08/2005

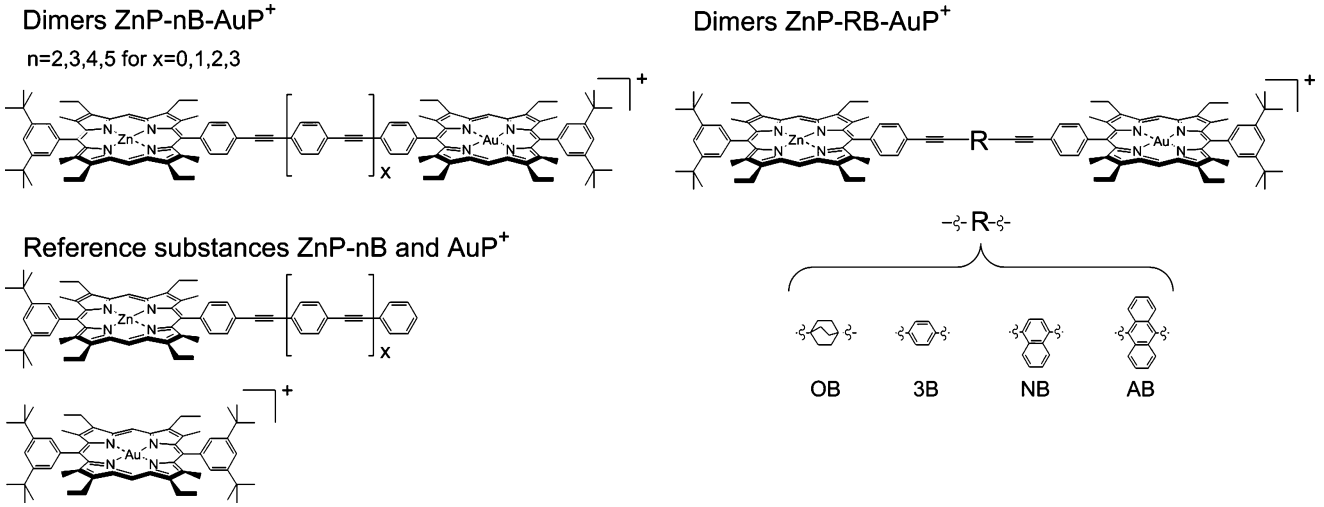

Figure 2. Structure of the dimers ZnP−nB−AuP$^+$ and ZnP−RB−AuP$^+$ and the reference substances ZnP−nB and AuP$^+$.

variation of the barrier height of the bridges.[13] That is, the electron transfer rate was shown to be dependent on the electronic properties of the bridges. For instance, we saw a correlation between the inverse energy splitting between the singlet excited states of the donor and the π-conjugated bridges (ΔE_{DB}) and the electronic coupling (V) between the donor and acceptor in accordance with the superexchange mechanism. The energy splitting ΔE_{DB} was estimated to be 17 600, 11 600, 8600, and 3900 cm^{-1} for OB, 3B, NB, and AB, respectively. Actually, electron transfer was unmeasurably slow in ZnP−OB−AuP$^+$, the D−B−A molecule with the largest ΔE_{DB}. Similarly, the electronic coupling was estimated to be 6.5 ± 1, 8.5 ± 1.5, and 14 ± 3 cm^{-1} for ZnP−RB−AuP$^+$ with the bridges 3B, NB, and AB, respectively. In summary, we concluded that V is strongly correlated to the inverse energy splitting (ΔE_{DB}) exactly as expected for the quantum mechanical tunneling probability. However, by minimizing ΔE_{DB} the possibility for a sequential (charge hopping) electron transfer mechanism via the bridges is always present. For example, for ZnP−AB−AuP$^+$ in polar solvents both mechanisms are in operation simultaneously: sequential and direct superexchange-mediated electron transfer.[14] Another example of sequential electron transfer was reported by Wasielewski and co-workers for an interesting set of oligo-*p*-phenylenevinylene bridges between a tetracene donor and pyromellitimide acceptor.[6] In their article, the importance of energy matching the D−B−A system is discussed, and it is shown that a small enough ΔE_{DB} value gives rise to sequential electron transfer. Further, Guldi and co-workers have recently reported a series of energy matched D−B−A systems with similar oligo-*p*-phenylenevinylene bridges, a tetraphenylporphyrin donor, and a C_{60} fullerene acceptor, where only direct electron transfer is observed.[15]

Here we are interested in studying the distance dependence of electron transfer in a set of donor−acceptor systems similar to the ZnP−RB−AuP$^+$ system. Consequently, the 3B bridge is shortened with one phenylethynyl unit or extended with one or two units giving another series of molecules; ZnP−2B−AuP$^+$, ZnP−3B−AuP$^+$, ZnP−4B−AuP$^+$, and ZnP−5B−AuP$^+$, in short ZnP−nB−AuP$^+$ (Figure 2). The two series of molecules − ZnP−nB−AuP$^+$ and ZnP−RB−AuP$^+$ − with one common bridge 3B give an opportunity to study the distance dependence and energy splitting dependence of electron transfer simultaneously in a systematic way.

Materials and Methods

All measurements throughout this paper were made at room temperature.

Materials. The synthesis of the ZnP−nB−AuP$^+$ systems as well as the relevant reference compounds are described elsewhere.[9,16,17] All solvents − butyronitrile (C_3H_7CN), methylene chloride (CH_2Cl_2), *N*,*N*-dimethylformamide (DMF), and chloroform ($CHCl_3$) − were of analytical grade and used as purchased.

Ground-State Absorption Spectroscopy. Ground-state absorption spectroscopy was performed with a Cary 4 Bio spectrophotometer or a Jasco V-530 spectrophotometer. A ground-state absorption spectrum of all samples was recorded prior to all other measurements to establish the purity and to determine the absorbance.

Steady-State Fluorescence Spectroscopy. The fully corrected emission spectra were recorded with a SPEX Fluorolog 3 or a SPEX Fluorolog τ2 spectrofluorimeter. The absorbance at the excitation wavelength was kept low, approximately 0.05 (corresponding to a concentration of approximately 2.5 μM), to avoid inner filter effects and intermolecular interactions. The systems were excited at the maximum of the donor Q-band absorption (538−548 nm, depending on solvent).

Time-Resolved Fluorescence Spectroscopy. Time-resolved fluorescence spectroscopy was carried out using the time-correlated single photon counting (TCSPC) method. An optical parametric oscillator (KTP−OPO, GWU) was pumped by a picosecond Ti:sapphire laser (Tsunami, Spectra Physics) that in turn was pumped by a continuous-wave frequency-doubled diode-pumped Nd:YVO4 laser (Millennia Pro, Spectra Physics). The 82 MHz output from the KTP−OPO at 1160 nm was acoustooptically modulated to 8 MHz by a pulse selector (Spectra Physics) and frequency-doubled in a BBO crystal. The excitation wavelength was kept at 580−582 nm (solvent-dependent), where the donor, ZnP, dominates the absorption. The sample response was recorded through a polarizer at the magic angle and a monochromator set at 633−643 nm (solvent-dependent) to record the donor ZnP emission. The photons were collected by a microchannel plate photomultiplier tube (MCP-PMT R3809U-50, Hamamatsu) and fed into a multichannel analyzer with 4096 channels. A diluted silica sol scattering solution was used to collect the instrument response signal. Further, the collected crude decay curves were iteratively convoluted and evaluated using the software package F900 (Edinburgh Instruments). The time resolution after deconvolu-

tion was about 10 ps (full width at half maximum). The decays were first fitted to a single-exponential model. The goodness of fit was evaluated by χ_R^2, the residuals, and by visual examination of the fitted decay. If the single-exponential decay was not satisfying, a second exponential decay and possibly a third exponential decay were used to fit the data. Most of the decay curves of ZnP−nB could be fitted satisfactorily to a single exponential, but in some cases a biexponential expression with a small preexponential factor (<0.1 normalized) was required. For the ZnP−nB−AuP^+ system at least a biexponential expression was required. The second time constant had a small preexponential factor and was equal to the unquenched ZnP time constant. For some decay curves of ZnP−nB−AuP^+ a third exponential was necessary, with a small preexponential factor (<0.1 normalized). In all TCSPC experiments the absorption at the excitation wavelength was set to 0.1−0.2.

Femtosecond Transient Absorption. For femtosecond transient absorption measurements the pump−probe technique was employed. The sample was excited at 573−580 nm (depending on solvent) where the donor ZnP dominates the absorption with the second harmonic of the signal from a TOPAS (Light Conversion Ltd.). The TOPAS was pumped by a Ti:sapphire regenerative amplifier (Spitfire, Spectra Physics) at 1 kHz repetition rate. The regenerative amplifier was pumped by a frequency-doubled diode-pumped Nd:YLF laser (Evolution-X, Spectra Physics) and seeded by a mode-locked femtosecond Ti: sapphire laser (Tsunami, Spectra Physics). The seed laser was pumped by a continuous-wave frequency-doubled diode-pumped Nd:YVO_4 laser (Millennia Vs, Spectra Physics). Further, the output from the regenerative amplifier (∼130 fs) was split into two beams with a beam splitter (70/30), the pump beam, and the probe beam. The pump beam (the output from the TOPAS) was chopped at 500 Hz to block the pump every second pulse. Subsequently the pump beam was sent through a computer-controlled optical delay line (Aerotech) and then focused with reflective optics on the sample at a small angle relative to the probe beam. The polarization of the pump beam relative to the polarization of the probe beam was set to the magic angle by a Berek compensator (New Focus) and the pulse energy at the sample in a typical experiment was 1.4 μJ/pulse. The intensity of the probe beam was reduced by two neutral density filters (one OD = 4 and one variable 0−2), before it was focused into a thin sapphire plate to generate a white light continuum. A second beam splitter (50/50) was used to split the generated white light continuum into the probe and the reference beams. Both beams were focused on the sample, with the probe beam overlapping the pump beam. After the sample, both probe and reference beams were focused onto the slit of a computer-controlled monochromator (ISA, TRIAX 180). Three photodiodes were used to monitor the intensity of probe, reference, and pump beams, respectively. The signals were gated by boxcar integrators (SR250, Stanford Research Systems), fed into a PC-based AD card, and averaged by a LabView program. In some experiments a CCD spectrograph (Avantes) was used instead of the diodes. The CCD has the advantage of measuring a full spectrum at each delay time.

The sample was held in a wagging 1 or 2 mm path length cuvette, and the optical density at the excitation wavelength was kept at 0.4−1. The decay traces were fitted to a sum of exponentials with the Matlab software package. All samples were measured in dimethylformamide (DMF), whereas only ZnP−2B−AuP^+, and a reference substance were studied in the other solvents.

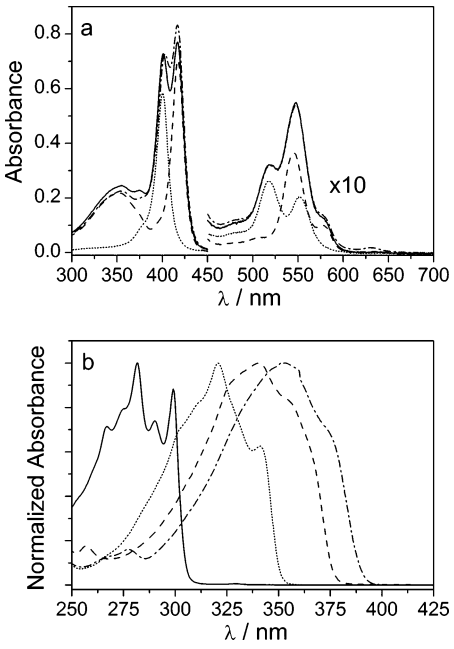

Figure 3. (a) Absorption spectra of ZnP−5B−AuP^+ (− · −) and the reference compounds ZnP−5B (--) and AuP^+ (···) in C_3H_7CN. The solid line spectrum (−) is the sum of the ZnP−5B and AuP^+ spectra. The Q-band region (>450 nm) is enlarged 10 times. (b) Absorption spectra of the bridges 5B (− · −), 4B (--), 3B (···), and 2B (−) in CH_2Cl_2.

Results

The purpose of this study is to investigate the influence of the bridge length on electron transfer. To do this, the photophysical properties of ZnP−nB−AuP^+ and the reference substances ZnP−nB and AuP^+ were investigated in four different solvents, CH_2Cl_2, $CHCl_3$, C_3H_7CN, and DMF. This section is organized as follows: First, ground-state absorption which was used to characterize the electronic structure of the ZnP−nB−AuP^+ system, is described. Second, steady-state emission and time-resolved emission are used to quantify the donor emission quenching. Finally, femtosecond transient absorption is used to confirm that the quenching was due to electron transfer.

Ground-State Absorption. Ground-state absorption was used to confirm that the ZnP−nB−AuP^+ systems consist of electronically separate chromophores. In Figure 3a it is shown that it is possible to resolve the ZnP−5B−AuP^+ spectrum into the reference spectra ZnP−5B and AuP^+; that is, the absorption spectrum of ZnP−5B and AuP^+ added together (solid line in Figure 3a) is almost identical to the absorption spectrum of ZnP−5B−AuP^+. The agreement in the porphyrin Q-band region (450−650 nm) is perfect, whereas there is a minor difference in the Soret-band region (350−450 nm).[9] Furthermore, the bridge molecules absorb below 400 nm separated from the porphyrin absorption. In Figure 3b the absorption spectra of the bridges can be compared. The excitation energy is lowest for the longest bridge and increases with decreasing bridge length.

Steady-State and Time-Resolved Fluorescence Spectroscopy. Steady-state and time-resolved fluorescence spectroscopy were used to give a quantitative description of the donor emission quenching. In Figure 4a the emission of ZnP−nB−AuP^+ can be compared to the emission of ZnP−2B; here only ZnP emission is seen since AuP^+ is nonfluorescent due to fast formation (240 fs) of a ligand-to-metal charge-transfer state.[18,19] Clearly, there is a large variation of donor emission quenching

TABLE 1: Fluorescence Lifetimes of the Molecules (τ), Rate Constant for Donor Emission Quenching (k), Calculated Förster Energy Transfer Rate Constant ($k_{\text{Förster}}$), and Rate Constant for Electron Transfer (k_{ET}) in C_3H_7CN at Room Temperature

	τ, ns	k,[a] s^{-1}	$k_{\text{Förster}}$, s^{-1}	k_{ET},[b] s^{-1}
ZnP−2B	1.411 ± 0.030			
ZnP−2B−AuP$^+$	0.025 ± 0.005	$(3.9 \pm 1.0) \times 10^{10}$	3.6×10^8	3.9×10^{10}
ZnP−3B	1.399 ± 0.030			
ZnP−3B−AuP$^+$	0.290 ± 0.050	$(2.7 \pm 0.7) \times 10^9$	6.1×10^{7} [c]	2.7×10^9
ZnP−4B	1.367 ± 0.030			
ZnP−4B−AuP$^+$	0.906 ± 0.050	$(3.7 \pm 0.8) \times 10^8$	1.5×10^7	3.6×10^8
ZnP−5B	1.415 ± 0.030			
ZnP−5B−AuP$^+$	1.222 ± 0.100	$(1.1 \pm 0.9) \times 10^8$	4.9×10^6	1.1×10^8

[a] Equation 3. [b] $k_{\text{ET}} = k - k_{\text{Förster}}$. [c] Previously reported to be 8×10^7 s^{-1};(ref 9) the deviation is due to that 25.3 Å was used as the center to center distance. This distance has now been calculated with higher accuracy to be 26.5 Å, see ref 39.

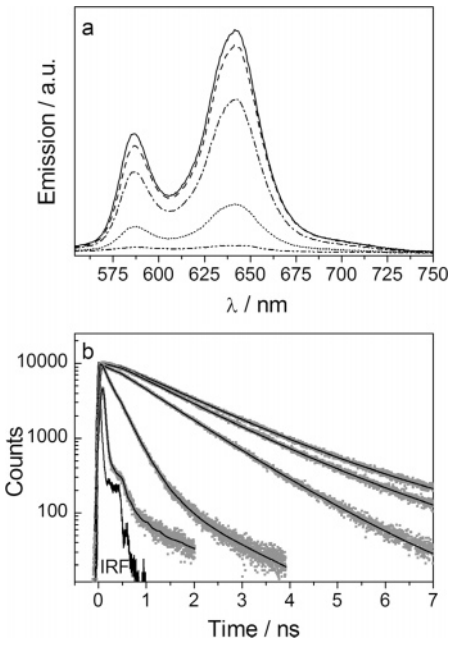

Figure 4. (a) Steady-state emission spectra of ZnP−2B (−), ZnP−5B−AuP$^+$ (--), ZnP−4B−AuP$^+$ (− · −), ZnP−3B−AuP$^+$ (···), and ZnP−2B−AuP$^+$ (− ·· −), in C_3H_7CN. (b) Fluorescence decay traces of ZnP−2B and ZnP−nB−AuP$^+$ in C_3H_7CN. ZnP−2B exhibits the longest lifetime followed by a decrease in lifetime with decreasing bridge length that is ZnP−5B−AuP$^+$ to ZnP−2B−AuP$^+$. The black curves in the traces are exponential fittings. IRF is the instrument response function.

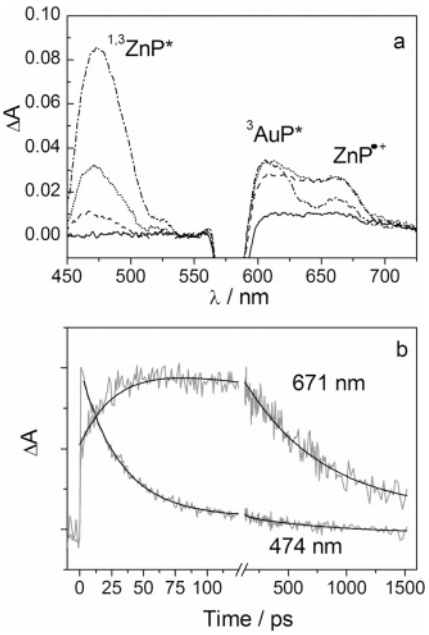

Figure 5. (a) Transient absorption spectra of ZnP−2B−AuP$^+$ in C_3H_7CN at 4 ps (− · −), 40 ps (···), 100 ps (--), and 1.3 ns (−). (b) Normalized kinetic traces at 474 and 671 nm for ZnP−2B−AuP$^+$ in C_3H_7CN.

depending on bridge length. The quenching increases with decreasing bridge length. The efficiency of the donor emission quenching in C_3H_7CN ($E = 1 - I_{\text{ZnP−nB−AuP}^+}/I_{\text{ZnP−nB}}$; I is emission intensity) is 0.07, 0.31, 0.77, and 0.97 for ZnP−nB−AuP$^+$ with $n = 5$, 4, 3, and 2, respectively. It will be demonstrated further on that electron transfer is the major deactivation channel in these systems.

In Figure 4b it is demonstrated how the lifetime decreases as the bridge length decreases. The efficiency of donor emission quenching in C_3H_7CN estimated from the time-resolved measurements ($E = 1 - \tau_{\text{ZnP−nB−AuP}^+}/\tau_{\text{ZnP−nB}}$) is 0.14, 0.31, 0.77, and 0.98 for ZnP−nB−AuP$^+$ with $n = 5$, 4, 3, and 2, respectively, in fair agreement with the steady-state emission measurements for the dimers with bridges 2B, 3B, and 4B. The deviations for ZnP−5B−AuP$^+$ can probably be explained by larger uncertainties in the relative difference in lifetimes of ZnP−5B−AuP$^+$ and ZnP−5B. By measuring the lifetime of ZnP−nB ($\tau_{\text{ZnP−nB}}$) and ZnP−nB−AuP$^+$ ($\tau_{\text{ZnP−nB−AuP}^+}$) (eqs 1 and 2) the quenching rate constant k can be calculated assuming that the intrinsic rate constants of the donor, such as intersystem crossing (k_{isc}), internal conversion (k_{ic}), and fluorescence (k_{f}), are unchanged when the acceptor is present. Since the structure of the ZnP absorption and emission spectra do not change in the presence of AuP$^+$, this assumption is likely to hold.

$$\tau_{\text{ZnP−nB}} = (k_{\text{ic}} + k_{\text{isc}} + k_{\text{f}})^{-1} \quad (1)$$

$$\tau_{\text{ZnP−nB−AuP}} = (k_{\text{ic}} + k_{\text{isc}} + k_{\text{f}} + k)^{-1} \quad (2)$$

$$k = (\tau_{\text{ZnP−nB−AuP}})^{-1} - (\tau_{\text{ZnP−nB}})^{-1} \quad (3)$$

The lifetimes and calculated quenching rate constants (eqs 1−3) are given in Table 1. The lifetime of the dimer increases with bridge length and is here shown to be 25 ps for ZnP−2B−AuP$^+$ and 1.2 ns for ZnP−5B−AuP$^+$. The lifetime of the longest dimer is thus close to the 1.4 ns lifetime of the reference substances. Table 1 is treated further in the discussion section.

Femtosecond Transient Absorption. Femtosecond transient absorption was used to verify that the quenching was caused by electron transfer. The key is to study the formation of the radicals, ZnP$^{\bullet+}$ and AuP$^{\bullet}$, which both are products of the electron transfer process. The main feature to look for is the radical cation (ZnP$^{\bullet+}$) that absorbs around 670−680 nm since AuP$^{\bullet}$ could not be distinguished among the other peaks in the spectrum. Characteristic ZnP/AuP$^+$ transient absorption spectra are seen in Figure 5a.[9,20] Strong singlet absorption dominates the spectra between 450 and 550 nm. Further, even though we minimized the AuP$^+$ excitation by exciting at 574 nm (in C_3H_7-

TABLE 2: Refractive Index (n), Dielectric Constant (ϵ), Excitation Energy (0−0 Transition, E_{00}), Calculated Reorganization Energy ($\lambda_{ZnP-nB-AuP^+}$), Calculated Driving Force ($\Delta G°$), and Damping Factor Beta (β) in Different Solvents at Room Temperature

solvent	n	ϵ	E_{00}, eV	$\lambda_{ZnP-2B-AuP^+}$, eV	$\lambda_{ZnP-3B-AuP^+}$, eV	$\lambda_{ZnP-4B-AuP^+}$, eV	$\lambda_{ZnP-5B-AuP^+}$, eV	$\Delta G°$, eV	β, Å^{-1}
$CHCl_3$	1.446	4.807	2.15	0.81	0.86	0.89	0.91	−0.43	0.25
CH_2Cl_2	1.424	8.93	2.15	1.06	1.14	1.18	1.21	−0.72	0.31
C_3H_7CN	1.384	24.83	2.13	1.29	1.38	1.44	1.47	−0.92	0.29
DMF	1.431	38.25	2.12	1.25	1.34	1.39	1.42	−0.95	0.31

CN, minor variation in other solvents) AuP^+ excited-state absorption dominates around 600 nm.[18,19] Around 680 nm the formation of $ZnP^{\bullet+}$ can be seen.[21−24] A negative contribution from stimulated emission is seen at 640 nm. At 575 nm we see ground-state bleaching coinciding with the scattered pump light. The spectrum is distorted between 520 and 560 nm and below 450 nm, due to complete absorption of the probe light.[25] The kinetic traces for ZnP−2B−AuP^+ at 671 and 474 nm (Figure 5b) show a buildup and decay in 27 and 30 ps, respectively. Accordingly, the formation of $ZnP^{\bullet+}$ is directly linked to the decay of ZnP singlet excited state. The formation and decay rates are in agreement with the fluorescence lifetime (25 ps) measured with TCSPC. We believe that the detection of the $ZnP^{\bullet+}$ formation is a solid proof of electron transfer. A similar result is found for ZnP−3B−AuP^+; the decay rate of the ZnP singlet excited state and the formation of $ZnP^{\bullet+}$ are in agreement with the fluorescence lifetime. For the ZnP−4B−AuP^+ and ZnP−5B−AuP^+ the formation of $ZnP^{\bullet+}$ is covered in the spectrum by the singlet absorption of ZnP as they evolve on the same time scale. For ZnP−4B−AuP^+ a small increase in ΔA at delay times longer than 1000 ps indicates that the radical state remains after the fluorescence has decayed. Further, the radical peak of ZnP−5B−AuP^+ is not detectable, and the decay at 671 nm shows features similar to the reference substance. However, this does not imply that electron transfer does not take place. The quenching has already proven to be small ($E \approx 0.1$), making the radical peak very hard to detect. At longer times the $ZnP^{\bullet+}$ peak decays due to the recombination reaction (Figure 5b) and the details of this will be treated elsewhere.[26]

Discussion

This section is divided into three parts: First it is established that electron transfer is the principal deactivation channel in the ZnP−nB−AuP^+ series. Second, the electronic couplings for the ZnP−nB−AuP^+ series are calculated. Finally the distance and bridge energy dependence are considered. Further, all through this section results are compared with measurements of the ZnP−RB−AuP^+ series, which is a well-defined system highly suitable for studying the bridge energy dependence of electron transfer.[9] With the ZnP−nB−AuP^+ series we incorporate the length dependence into a full description of electron transfer, taking both the electronic properties and the length of the bridges into account.

Electron Transfer. Electron transfer is the dominant deactivation channel in ZnP−nB−AuP^+. In the transient absorption spectra there is a clear signal for the $ZnP^{\bullet+}$, which is a product of electron transfer. Still there might be a small contribution of excitation energy transfer present, and to investigate this, the contribution of Förster energy transfer is calculated. The Förster energy transfer rate is calculated[27] to be 4.9×10^6 s^{-1} for ZnP−5B−AuP^+ and increases with decreasing distance to 3.6×10^8 s^{-1} for ZnP−2B−AuP^+, see Table 1. It can be seen that the electron transfer rate is more than 1 order of magnitude larger than the calculated Förster energy transfer rate for all systems, and thus, energy transfer should only make a minor contribution to the donor emission quenching.

Further, in parallel to this project we are studying energy transfer in a ZnP−nB−H_2P series, where the only difference from ZnP−nB−AuP^+ is that AuP^+ is exchanged to an energy-accepting free base porphyrin.[28] In this study we show that the energy transfer rate is substantially larger than the Förster energy transfer rate due to the so-called "bridge mediation effect". Assuming that the mediation contribution is on the same order of magnitude when AuP^+ is the acceptor, electron transfer is still the dominating deactivation channel in all dimers. As the donor−acceptor overlap is much larger for ZnP/H_2P than for ZnP/AuP^+ the energy transfer mediation contribution in ZnP−nB−AuP^+ is probably much smaller than in ZnP−nB−H_2P. On the whole, electron transfer is the major mechanism of the donor emission quenching in the ZnP−nB−AuP^+ series.

Calculating the Electronic Coupling. According to the classical Marcus theory the electron transfer rate constant is described as

$$k_{ET} = \sqrt{\frac{\pi}{\hbar^2 \lambda k_B T}} |V|^2 \exp\left(\frac{-(\Delta G° + \lambda)^2}{4\lambda k_B T}\right) \qquad (4)$$

where V is the electronic coupling between the donor and acceptor, λ is the total reorganization energy, T is the temperature, k_B is the Boltzmann constant, and h is the Planck constant ($\hbar = h/2\pi$).[29−31] The driving force, $\Delta G°$, can be calculated from the measured redox potentials[32−35]

$$\Delta G° \text{ (eV)} = e(E_{ox} - E_{red}) - E_{00} + \frac{e^2}{4\pi\epsilon_0 r}\left(\frac{1}{\epsilon_s} - \frac{1}{\epsilon_s^{ref}}\right) \qquad (5)$$

where E_{ox} (0.38 V)[9,36] and E_{red} (−1.05 V)[9,36] are the donor and acceptor oxidation and reduction potentials, respectively. In Table 2, E_{00}, the energy of the 0−0 transition of the donor determined from the midpoint between the absorption and emission spectra, are given together with ϵ_s, the dielectric constant of the solvent. ϵ^{ref}_s is the dielectric constant of the solvent in which the cyclic voltammetry measurements were performed; r is the average radius (4.8 Å)[9,37] of the porphyrins. Usually a Coulombic stabilization term is present in eq 5, but since the electron transfer process can be described as a charge shift (ZnP*−nB−AuP^+ → $ZnP^{\bullet+}$−nB−$AuP^{\bullet}$) rather than charge separation, this term has been omitted. In any case, $\Delta G°$ changes less than 0.1 eV if this term is included.

Theoretical values of λ can be estimated using the dielectric continuum model[32−35]

$$\lambda = \lambda_i + \lambda_o = \lambda_i + \frac{e^2}{4\pi\epsilon_0}\left(\frac{1}{r} - \frac{1}{R_{cc}}\right)\left(\frac{1}{n^2} - \frac{1}{\epsilon_s}\right) \qquad (6)$$

where λ_i and λ_o are the inner and outer (solvent) reorganization energies, respectively. R_{cc} is the center to center distance between donor and acceptor (Table 3), and n is the refractive index of the solvent (Table 2). The inner reorganization energy is set to 0.2 eV, which has been used previously for ZnP/AuP^+ donor acceptor pairs.[9,38] In Table 2 the calculated λ and $\Delta G°$

TABLE 3: Center to Center Distance (R_{cc}), Edge to Edge Distance (R_{ee}), Energy Splitting between the Singlet Excited States of the Donor and Bridge (ΔE_{DB}), and Experimentally Determined Electronic Coupling (V)

	R_{ee},[a] Å	R_{cc},[a] Å	ΔE_{DB}, cm^{-1}	V, cm^{-1}
ZnP−2B−AuP$^+$	12.7	19.7	15 800	18.8 ± 3.4
ZnP−3B−AuP$^+$	19.6	26.5	11 600	6.7 ± 0.9
ZnP−4B−AuP$^+$	26.5	33.4	9 700	4.4 ± 2.2
ZnP−5B−AuP$^+$	33.4	40.3	8 800	1.5 ± 0.5

[a] Distances reported in Eng et al.[39]

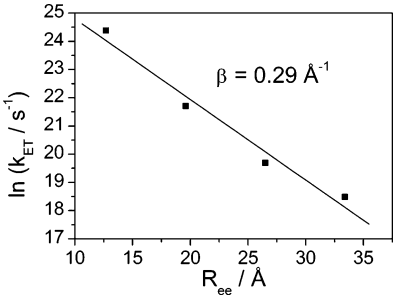

Figure 6. ln k versus the edge to edge distance R_{ee} for ZnP−nB−AuP$^+$ in C_3H_7CN.

for ZnP−nB−AuP$^+$ are presented, and it can be seen that the electron transfer process is in the Marcus normal region, that is, $-\Delta G° < \lambda$ for all solvents and all distances. The total reorganization energy has a minor distance dependence; for example in C_3H_7CN it is 1.29 eV for the dimer with the 2B bridge and 1.47 eV for the 5B bridge. There is a larger variation between solvents with different polarity, and in $CHCl_3$ the total reorganization energy of ZnP−2B−AuP$^+$ is 0.81 eV and in DMF 1.25 eV. The driving force is negative for all solvents, implying an exergonic electron transfer process.

The Marcus equation (eq 4) is used to estimate V for each dimer in all four solvents. The average for each dimer is listed in Table 3. The estimated V varies between 1.5 cm^{-1} for ZnP−5B−AuP$^+$ and 19 cm^{-1} for ZnP−2B−AuP$^+$. The magnitude of V is in good agreement with previous measurements.[9]

Distance and Bridge Energy Dependence. Both the direct electronic coupling and the superexchange coupling have exponential distance dependence.[2] As the rate constant for electron transfer is proportional to the squared coupling by the Fermi Golden rule, the distance-dependent electron transfer data are usually analyzed with an exponential expression:[2]

$$k_{ET}(R) = k_0 \exp(-\beta R_{ee}) \tag{7}$$

R_{ee} is the (edge to edge) distance between donor and acceptor, and k_0 is the hypothetical rate at contact distance. The damping factor β is usually considered to be a bridge-specific factor.

The damping factor β (see Table 2) is determined for each solvent respectively by plotting ln k versus the edge to edge distance, R_{ee}. The average of β is 0.29 ± 0.04 Å^{-1}, and the variation between solvents is within the experimental error. In Figure 6 the distance dependence for the ZnP−nB−AuP$^+$ series in C_3H_7CN is shown, and although the fit is quite good, a slight upward curvature may be noted. It is also possible to determine β using estimated V (Table 3), by plotting ln V^2 versus R_{ee}. This β value, is estimated to be 0.23 Å^{-1}. The difference between the two βs is probably explained by the uncertain estimation of λ and $\Delta G°$ (eqs 5 and 6).

β values for electron transfer have been reported for many different conjugated bridges of which only a few examples will be mentioned, $\beta = 0.03$ Å^{-1} for p-phenylenevinylene bridges,[15] $\beta = 0.10$ Å^{-1} for polyyne bridges,[5] $\beta = 0.08$ Å^{-1} for polyene bridges,[5] and $\beta = 0.4$ Å^{-1} for polyphenylene bridges.[4] For oligo-p-phenyleneethynylene (OPE) bridges (the nB bridges), both experimentally and theoretically determined β values have been reported. For example, for OPE bridges in a monolayer-based electrochemical system Creager et al.[40] reports β values of 0.36 Å^{-1} and Sachs et al.[41] reports 0.57 Å^{-1}. Furthermore, Sachs et al. theoretically determined β to be 0.4 Å^{-1} for completely planar OPE bridges, 1.0 Å^{-1} for bridges where the phenyl units are orthogonal, that is minimum π-conjugation, and 0.5 Å^{-1} for a uniform distribution of conformations in the OPE bridge.[41] For the same bridge in a planar conformation Magoga and Joachim report 0.28 Å^{-1} on the basis of electron scattering calculations,[42] and Larsson and Klimkāns calculated β to be 0.30 Å^{-1} with the CNDO/S method.[43] In the experimental determinations of the distance dependence, it is imperative to identify the cases where a hopping mechanism is possible, since with this mechanism the β values are expected to be much smaller, and, actually, the distance dependence is not even expected to be exponential. In our opinion, only true cases of superexchange-mediated or direct electron transfer should be characterized with a β value.

By using perturbation theory, McConnell derived an expression for the relation of the electronic coupling (V_{DA}) between donor and acceptor and the energy splitting between the relevant states of the donor and bridge (ΔE_{DB}),[1]

$$V_{DA} = \frac{V_{DB}V_{BA}}{\Delta E_{DB}} \tag{8}$$

For electron transfer, the value of ΔE_{DB} should be given by the LUMO energy difference between the bridge and donor. It has been shown for these systems that ΔE_{DB} can be estimated from the energy gap between the unrelaxed singlet excited states; that is, $\Delta E_{DB} = E_{00}^{B} - E_{00}^{D}$.[9] It has been common to estimate this energy gap from electrochemical data (first reduction and excited-state oxidation potentials for the bridge and donor molecules, respectively), but this procedure was shown in ref 9 to fail for the ZnP−RB−AuP$^+$ series. As an alternative we suggested estimatation of the variation of ΔE_{DB} from the difference in the excited-state energies of the bridge and donor chromophores. This is valid for chromophores such as the OPE bridges, which have the lowest singlet excited states that are dominated by a simple HOMO−LUMO configuration and a LUMO energy proportional to the energy of the first excited state.[44] It should be noted that the relative magnitude of ΔE_{DB} rather than the absolute value of the energy gap is estimated in this way. A linear dependence between V_{DA} and $1/\Delta E_{DB}$ was proven for ZnP−RB−AuP$^+$ [9] with a slope $V_{DB}V_{BA}$ of 74 000 cm^{-2}, which shows that the electronic coupling is strongly correlated to the inverse energy splitting. In the ZnP−nB−AuP$^+$ series we change both ΔE_{DB} and the donor−acceptor separation at the same time. As the length of the nB bridges increases, ΔE_{DB} decreases, and a positive deviation from the exponential distance dependence is expected for the ZnP−nB−AuP$^+$ series due to the ΔE_{DB} dependence. As shown in the β plot (Figure 6), the data for ZnP−nB−AuP$^+$ fits quite well to exponential distance dependence, although a slight positive deviation is noted. The lack of deviation from the exponential dependence is explained by the following: first, ΔE_{DB} is quite large for the dimers with nB bridges compared to the AB-bridged system, and second, the variation of ΔE_{DB} among the dimers with nB bridges is small (ΔE_{DB} = 15 800 cm^{-1} for ZnP−2B−AuP$^+$ and 8800 cm^{-1} for ZnP−5B−AuP$^+$ compared to 17 600 cm^{-1} for ZnP−OB−AuP$^+$ and 3900 cm^{-1} for ZnP−AB−AuP$^+$). To

make a crude estimate of how V_{DA} would vary in the ZnP−nB−AuP$^+$ series if the length dependence was absent, the expected variation is calculated from eq 8 using the known slope from the ZnP−RB−AuP$^+$ series. Again, we believe that this is valid due to the similarities of the two systems. The resulting V_{DA} varies between 4.7 and 8.4 cm^{-1} for the 2B, 3B, 4B, and 5B dimers. But as the experimentally determined V varies from 1.5 to 19 cm^{-1} for the ZnP−nB−AuP$^+$ series, it is found that the length dependence is much stronger than the energy splitting dependence in this case. If ΔE_{DB} would have been smaller and/or the variation in ΔE_{DB} larger, the deviation from linear dependence would be expected to be stronger. In fact, considering the systems with much smaller β values mentioned earlier for different conjugated bridges, the relative amount of bridge energy dependence is probably significantly larger. Finally, since the damping factor, β, is a function of the energy splitting between the donor and the conjugated bridge (ΔE_{DB}), each specific donor−bridge−acceptor system will have a unique β. In a series where the variation in ΔE_{DB} is small an exponential fall-off with distance is expected, but when the variation is large, the deviation might be substantial. In addition, β is not expected to be the same for a given bridge since the specific donor and acceptors appended to the bridge also influence the distance dependence. This is seen quite clearly when comparing the scattered results that have been determined for the OPE bridges in different systems.[40−43]

Conclusions

The electron transfer process in the ZnP−nB−AuP$^+$ systems has been verified by detection of formation and decay of the zinc porphyrin radical cation with femtosecond transient absorption spectroscopy. The efficiency of electron transfer, based on time-resolved fluorescence measurements, was 0.98, 0.77, 0.31, and 0.14 in C_3H_7CN for ZnP−nB−AuP$^+$ with the edge to edge distance 12.7, 19.6, 26.5, and 33.4 Å (n = 2, 3, 4, and 5), respectively. Further, the electron transfer rate, which was studied in four solvents, showed exponential distance dependence and the damping factor β was determined to 0.29 ± 0.04 Å^{-1}. On the basis of the Marcus and Rehm−Weller equations, the electronic coupling between donor and acceptor was estimated to be 18.8 ± 3.4, 6.7 ± 0.9, 4.4 ± 2.2, and 1.5 ± 0.5 cm^{-1} for ZnP−nB−AuP$^+$ with n = 2, 3, 4, and 5, respectively.

Finally, we are discussing the importance of considering both the distance between donor−acceptor and ΔE_{DB} in D−B−A systems for electron transfer. We have already demonstrated for the ZnP−RB−AuP$^+$ series that the electron transfer rate is inversely proportional to ΔE_{DB}. Here we show that the distance dependence is significantly stronger than the ΔE_{DB} dependence for the ZnP−nB−AuP$^+$ series. It is common to consider only the distance dependence when analyzing electron transfer data, but, as has been shown, the electron transfer rate will also depend on the barrier height, ΔE_{DB}. This is particularly important when ΔE_{DB} is small or exhibits large variations with the bridge length. Hence, when designing a functional electron transfer system the effects of varying ΔE_{DB} should also be considered.

Acknowledgment. This work was supported by grants from the Swedish Research Council, the Knut and Alice Wallenberg Foundation, and the Hasselblad Foundation.

References and Notes

(1) McConnell, H. M. *J. Chem. Phys* **1961**, *35*, 508−515.
(2) Closs, G. L.; Miller, J. R. *Science* **1988**, *240*, 440−447.
(3) Paddon-Row, M. N.; Oliver, A. M.; Warman, J. M.; Smit, K. J.; De Haas, M. P.; Oevering, H.; Verhoeven, J. W. *J. Phys. Chem.* **1988**, *92*, 6958−6962.
(4) Helms, A.; Heiler, D.; McLendon, G. *J. Am. Chem. Soc.* **1992**, *114*, 6227−6238.
(5) Osuka, A.; Tanabe, N.; Kawabata, S.; Yamazaki, I.; Nishimura, Y. *J. Org. Chem.* **1995**, *60*, 7177−7185.
(6) Davis, W. B.; Svec, W. A.; Ratner, M. A.; Wasielewski, M. R. *Nature* **1998**, *396*, 60−63.
(7) Portela, C. F.; Brunckova, J.; Richards, J. L.; Schollhorn, B.; Iamamoto, Y.; Magde, D.; Traylor, T. G.; Perrin, C. L. *J. Phys. Chem. A* **1999**, *103*, 10540−10552.
(8) Heitele, H.; Michel-Beyerle, M. E.; Finckh, P. *Chem. Phys. Lett.* **1987**, *134*, 273−278.
(9) Kilså, K.; Kajanus, J.; Macpherson, A. N.; Mårtensson, J.; Albinsson, B. *J. Am. Chem. Soc.* **2001**, *123*, 3069−3080.
(10) Brun, A. M.; Harriman, A.; Heitz, V.; Sauvage, J. P. *J. Am. Chem. Soc.* **1991**, *113*, 8657−8663.
(11) Flamigni, L.; Armaroli, N.; Barigelletti, F.; Chambron, J.-C.; Sauvage, J.-P.; Solladie, N. *New J. Chem.* **1999**, *23*, 1151−1158.
(12) Andersson, M.; Linke, M.; Chambron, J.-C.; Davidsson, J.; Heitz, V.; Sauvage, J.-P.; Hammarström, L. *J. Am. Chem. Soc.* **2000**, *122*, 3526−3527.
(13) Previously we have reported 25.3 Å, but more sophisticated methods estimate the distance to be 26.5 Å; see ref 39.
(14) Winters, M. U.; Pettersson, K.; Mårtensson, J.; Albinsson, B. *Chem. Eur. J.* **2005**, *11*, 562−573.
(15) De la Torre, G.; Giacalone, F.; Segura, J. L.; Martin, N.; Guldi, D. M. *Chem. Eur. J.* **2005**, *11*, 1267−1280.
(16) Ljungdahl, T.; Pettersson, K.; Albinsson, B.; Mårtensson, J. Submitted for publication in *J. Org. Chem.*
(17) Kajanus, J.; van Berlekom, S. B.; Albinsson, B.; Mårtensson, J. *Synthesis* **1999**, 1155−1162.
(18) Eng, M. P.; Ljungdahl, T.; Andréasson, J.; Mårtensson, J.; Albinsson, B. *J. Phys. Chem. A* **2005**, *109*, 1776−1784.
(19) Andréasson, J.; Kodis, G.; Lin, S.; Moore, A. L.; Moore, T. A.; Gust, D.; Mårtensson, J.; Albinsson, B. *Photochem. Photobiol.* **2002**, *76*, 47−50.
(20) Andréasson, J.; Kodis, G.; Ljungdahl, T.; Moore, A. L.; Moore, T. A.; Gust, D.; Mårtensson, J.; Albinsson, B. *J. Phys. Chem. A* **2003**, *107*, 8825−8833.
(21) Kilså, K.; Macpherson, A. N.; Gillbro, T.; Mårtensson, J.; Albinsson, B. *Spectrochim. Acta, Part A* **2001**, *57*, 2213−2227.
(22) Imahori, H.; Hagiwara, K.; Aoki, M.; Akiyama, T.; Taniguchi, S.; Okada, T.; Shirakawa, M.; Sakata, Y. *J. Am. Chem. Soc.* **1996**, *118*, 11771−11782.
(23) Chosrowjan, H.; Tanigichi, S.; Okada, T.; Takagi, S.; Arai, T.; Tokumaru, K. *Chem. Phys. Lett.* **1995**, *242*, 644−649.
(24) Pettersson, K.; Kilså, K.; Mårtensson, J.; Albinsson, B. *J. Am. Chem. Soc.* **2004**, *126*, 6710−6719.
(25) This is a consequence of high absorption in these regions because we excite at 574 nm to minimize the AuP absorption. Therefore the absorption in the mentioned areas are very high as the extinction coefficient is much larger at these wavelengths; see the absorption spectrum in Figure 3a.
(26) Wiberg, J.; Pettersson, K.; Mårtensson, J.; Albinsson, B. Work in progress.
(27) Since the donor and acceptor are exactly the same as in ZnP−RB−AuP$^+$, the same sets of parameters are used, with the exception of the donor−acceptor distance; see ref 9 for details.
(28) Pettersson, K.; Kyrychenko, A.; Rönnow, E.; Ljungdahl, T.; Mårtensson, J.; Albinsson, B. *J. Phys. Chem. B.*, in press.
(29) Marcus, R. A. *J. Chem. Phys.* **1956**, *24*, 966−978.
(30) Levich, V. G. In *Advances in Electrochemisty and Electrochemical Engineering*; Delahay, P., Ed.; Interscience: New York, 1966; Vol. 4, pp 249−371.
(31) Marcus, R. A.; Sutin, N. *Biochim. Biophys. Acta* **1985**, *811*, 265−322.
(32) Marcus, R. A. *Can. J. Chem.* **1959**, *37*, 155−163.
(33) Marcus, R. A. *J. Chem. Phys.* **1965**, *43*, 679−701.
(34) Rehm, D.; Weller, A. *Ber. Bunsen-Ges. Phys. Chem.* **1969**, *73*, 834−839.
(35) Weller, A. *Z. Phys. Chem. (Muenchen)* **1982**, *133*, 93−98.
(36) Versus an Ag/Ag$^+$ electrode (E = 0.45 versus SHE).
(37) DeGraziano, J. M.; Macpherson, A. N.; Liddell, P. A.; Noss, L.; Sumida, J. P.; Seely, G. R.; Lewis, J. E.; Moore, A. L.; Moore, T. A.; Gust, D. *New J. Chem.* **1996**, *20*, 839−851.
(38) Harriman, A.; Heitz, V.; Sauvage, J. P. *J. Phys. Chem.* **1993**, *97*, 5940−5946.
(39) Eng, M. P.; Ljungdahl, T.; Mårtensson, J.; Albinsson, B. Submitted for publication in *J. Phys. Chem. B.*

(40) Creager, S.; Yu, C. J.; Bamdad, C.; O'Connor, S.; MacLean, T.; Lam, E.; Chong, Y.; Olsen, G. T.; Luo, J.; Gozin, M.; Kayyem, J. F. *J. Am. Chem. Soc.* **1999**, *121*, 1059−1064.

(41) Sachs, S. B.; Dudek, S. P.; Hsung, R. P.; Sita, L. R.; Smalley, J. F.; Newton, M. D.; Feldberg, S. W.; Chidsey, C. E. D. *J. Am. Chem. Soc.* **1997**, *119*, 10563−10564.

(42) Magoga, M.; Joachim, C. *Phys. Rev. B: Condens. Matter Mater. Phys.* **1997**, *56*, 4722−4729.

(43) Larsson, S.; Klimkāns, A. *J. Mol. Struct.* **1999**, *464*, 59−65.

(44) The singlet excited-state energies of all the different bridges (RB and nB) are found to be proportional to their first reduction potentials.